COMPRESSIVE STRENGTH AND BEHAVIOR ANALYSIS OF FULL-SCALE CONCRETE FILLED STEEL TUBULAR COLUMNS

Hao Dinh Phan, Ve Van Thi, Tuan Cao Le*, Luan Hung Tran

The University of Danang – University of Science and Technology, Vietnam

*Corresponding author: lctuan@dut.udn.vn

(Received: May 02, 2025; Revised: June 10, 2025; Accepted: June 23, 2025)

DOI: 10.31130/ud-jst.2025.23(10C).666E

Abstract - This paper investigates the compressive behavior of full-scale concrete filled steel tubular (CFST) columns with varying heights, loading conditions, and constituent material strengths. A numerical study was conducted on eighteen CFST specimens with steel yield strengths (f_y) ranging from 620 to 690 MPa and concrete compressive strengths (f_c') ranging from 80 to 100 MPa. Two concentric loading types were applied: over the entire cross-section (CFE) and on the concrete core only (CFC). Results indicate that both loading type and material strength significantly affect column performance. CFC-loaded columns achieved higher compressive strength but lower deformation capacity compared to those under CFE loading, due to variations in the confinement effect provided by the steel tube. Increasing f_y and f_c' enhanced overall column's compressive strength, while higher f_c' led to greater concrete core damage. The AS/NZS 2327: 2017 design standard provides conservative yet reliable strength predictions for CFST columns constructed with high strength materials.

Key words - Full-scale concrete filled steel tubular (CFST) columns; Finite element models (FEMs); High strength materials; Loading conditions; Confinement effects; AS/NZS 2327: 2017.

1. Introduction

Concrete filled steel tubular (CFST) columns are widely employed in high-rise buildings due to their notable advantages over conventional reinforced concrete (RC) columns. These advantages include higher strength, superior ductility, and shorter construction times. Consequently, the adoption of CFST columns is a logical trend to mitigate some of the inherent drawbacks of RC columns, such as heavy self-weight, large cross-sectional dimensions, low ductility, and slower construction processes.

CFST columns have been extensively studied and implemented in high-rise construction across many developed countries. Considerable research, analytical [1-5], experimental [2], [3], [5-8], and numerical [7], [9-19], has focused on understanding their compressive strength and structural behavior. These studies have primarily addressed key issues such as the axial capacity and overall behavior of CFST columns, local buckling of the steel tubes, the confinement effects on the concrete core, and the flexural performance of CFST beam-columns under various loading conditions.

Finite element analysis (FEA), facilitated by advanced simulation software, has become a widely adopted tool for investigating the mechanical behavior of CFST columns. Numerous researchers have used FEA to study the performance of CFST columns under different loading conditions. For axially loaded columns, prior research has demonstrated that both the cross-sectional shape and the width/diameter-to-thickness ratio (B/t or D/t) of the steel tube significantly influence the compressive strength and behavior of the columns [1], [13]. Columns with circular cross-sections generally exhibit superior confinement effects compared to non-circular sections. Moreover, the concrete core benefits most from confinement under axial compression compared to other loading types [2], [3], [9], [10], [12], [18].

To accurately simulate the complex interaction between steel tubes and infilled concrete, various material models have been adopted in prior studies [10], [11], [14-16]. Most of these investigations used materials with nominal strengths within the typical upper limits from 60 to 69 MPa for concrete compressive strength and 460 to 525 MPa for structural steel yield strength. However, some studies have extended beyond these ranges, exploring the performance of CFST columns using high strength materials. Advancing the use of high strength materials (above 69 MPa for concrete and 525 MPa for steel) is essential for optimizing the structural efficiency of CFST columns, especially in high-rise applications.

Although numerous models have been proposed to simulate CFST column behavior under axial loading, accurately capturing the behavior of confined concrete, particularly in full-scale columns using high strength materials, remains a significant challenge. Due to the limited availability of experimental data for full-scale specimens, this study conducts a comprehensive numerical investigation into the compressive strength and behavior of circular CFST columns using high strength materials, consistent with the upper limits specified in AS/NZS 2327: 2017 [20].

This paper presents the findings of these numerical analyses, with a primary focus on evaluating the influence of key parameters, such as column height, loading conditions, and constituent material strengths, on the compressive performance of full-scale CFST columns.

2. Numerical simulation program

2.1. CFST columns' modeling

In this study, ABAQUS [21], a commercial software based on the finite element method (FEM), was used to simulate the behavior of CFST columns using various material strengths under compressive loads across different loading cases. The simulation process encompasses all components of the CFST column specimens: the steel tube, concrete core, and loading plates.

To ensure accurate analysis, a mesh size convergence study was conducted to determine the optimal mesh sizes

for the steel tube and concrete core. In this investigation, a CFST column, designated C-CFE-620-80, was selected. The column comprises steel with a yield strength of 620 MPa and concrete with a compressive strength of 80 MPa, and was subjected to full cross-sectional loading. The results of the mesh convergence analysis are presented in Figure 1(a), which shows a negligible change of 0.13% in the column's compressive strength between mesh configurations 34-44 and 32-42. Based on the findings, a mesh size of 32x32 mm for the steel tube and 42x42 mm for the concrete core was adopted for the CFE loading case, as illustrated in Figure 1(b).

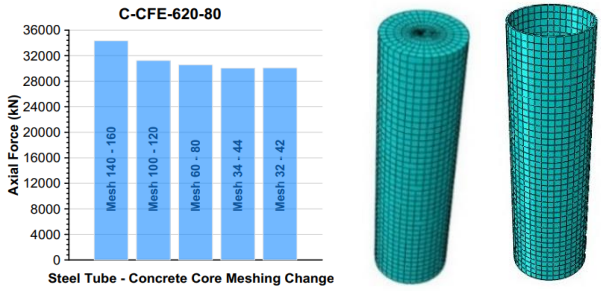

(a) Mesh convergence analysis *(b) Selected mesh size*

***Figure 1**. Meshing for concrete core and steel tube components*

To model the material properties of the steel tube in ABAQUS, an elasto-plastic model, as shown in Figure 2, is employed. In the elastic range, the stress-strain behavior is defined using a linear relationship based on the steel's modulus of elasticity (E_s) and yield strength (f_y). Specifically, the modulus of elasticity is taken as 200 GPa, and the Poisson's ratio (v_s) is assumed to be 0.3. The nominal yield strength f_y is used to represent the steel's initial yield point. In this study, the steel tubes have yield strengths of 620, 655, and 690 MPa.

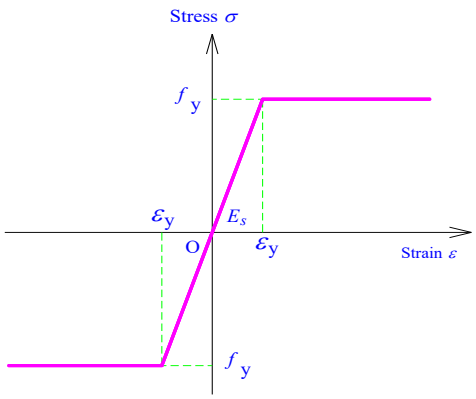

***Figure 2.** Elasto-plastic model for steel tube*

Developing a rational and accurate material model to simulate the behavior of concrete filled in CFST columns, especially for large-scale specimens, remains a significant challenge. This study adopts the Concrete Damaged Plasticity (CDP) model available in ABAQUS, enhanced to incorporate the effects of confinement provided by the steel tube. A confined concrete model, previously developed by the first author [18], is employed to better capture the compressive behavior of concrete within circular CFST columns. As illustrated in Figure 3, the proposed model is calibrated for concrete infill with compressive strengths (f'_c) of 80, 90, and 100 MPa, along with the corresponding yield strengths of the outer steel tube. Furthermore, this confined concrete model is updated with the actual concrete properties, enhancing the accuracy of the modeling results. In this process, key material factors in the CDP model, including the ratio of biaxial to uniaxial compressive strength (f_{b0}/f'_c), the ratio of the second stress invariant on the tensile meridian to that on the compressive meridian (K_c), the dilation angle (ψ), and the strain hardening/softening rule, were determined and calculated based on the formulations provided in Equations (1)-(4) below.

$$\frac{f_{b0}}{f'_c} = \frac{1.5}{f'^{(0.075)}_c} \quad (1)$$

$$K_c = \frac{5.5f_{b0}}{3f'_c + 5f_{b0}} = 5.5\frac{1}{5 + 2f'^{(0.075)}_c} \quad (2)$$

$$\psi = \begin{cases} 56.3(1-\xi_c)\ for\ \xi_c \le 0.5 \\ 6.672e^{\left(\frac{7.4}{4.64+\xi_c}\right)}\ for\ \xi_c > 0.5 \end{cases} \quad (3)$$

$$\xi_c = \frac{A_s f_y}{A_c f'_c} \quad (4)$$

where, f_{b0} denotes the biaxial compressive strength of concrete; A_s and A_c represent the cross-sectional areas of the steel tube and the concrete core, respectively; and ξ_c is the confinement factor.

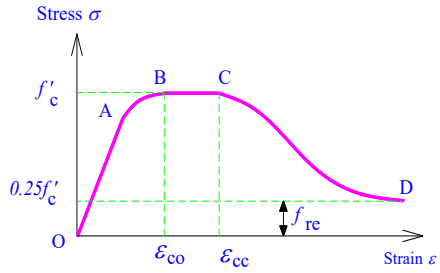

***Figure 3.** A confined concrete model [18]*

For modeling steel-concrete interaction in CFST columns, the *Contact Pair option with surface-to-surface contact type was used to represent the interaction between the inner surface of the steel tube and the outer surface of the concrete core. This contact pair involves defining a master surface and a slave surface. To minimize numerical errors, the slave surface is assigned to the softer component, which is the steel tube, and is usually meshed more finely than the master surface, which is the concrete core [21].

Contact behavior between the two surfaces was defined in both the normal and tangential directions. Normal contact behavior was modeled using the 'Hard' contact formulation, allowing separation after contact. Tangential behavior was defined using the Coulomb friction model, with the friction coefficient set to 0.25 for loading applied to the entire cross-section and 0.3 when the load was applied only to the concrete core cross-section (Figure 4) [12], [18]. The friction coefficients were selected based on values proposed in previous studies and the sensitivity analysis conducted in this study. The analysis revealed that the friction coefficient has a negligible impact on the modeling results.

This study considered two loading cases for CFST

column specimens: loading applied to the entire cross-section (CFE), and to the concrete core cross-section only (CFC). The geometric dimensions of the CFST column specimens, as well as the respective loading cases, are shown in Figure 4. To accurately simulate the real-life behavior of these columns, careful attention was given to the setup of boundary conditions and load application methods.

In the CFE loading case, two steel loading plates were used in the simulation to distribute the axial load uniformly across the entire cross-section. In contrast, for the CFC case, the axial compression load was applied directly to the surface of the concrete core. Boundary conditions and compressive loads were imposed at both ends of the columns using Reference Points (RPs). At the top end (RP1), the column was partially restrained, five degrees of freedom (DOFs) were fixed, while one DOF (translation along the longitudinal axis) was released to permit vertical movement. At the bottom end (RP2), the column was fully fixed, with all six DOFs constrained.

A displacement-controlled loading approach was adopted, with a maximum applied displacement of 45 mm, which was used consistently across all column specimens.

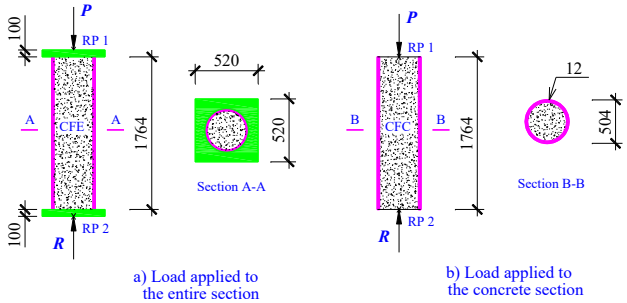

Figure 4. *Dimensions of CFST specimens and loading cases*

The finite element models (FEMs) of the various column specimens developed in this study utilized an elasto-plastic material model for the steel tube and a confined concrete model for the concrete core [18]. These models were validated against both experimental and numerical results from previous studies [2], [12], demonstrating good agreement with the findings reported in [19].

2.2. Parametric studies

To investigate the effect of column height, loading conditions, and constituent material strengths on the compressive strength and behavior of full-scale CFST columns, a series of parametric studies were conducted based on the developed finite element simulation. Specifically, the influence of column height was examined under both loading cases, CFE and CFC, by varying the column height (H) from 2.0D to 4.0D, where D denotes the outer diameter of the steel tube.

As shown in Figures 5 and 6, the results indicate that increasing the column height leads to a reduction in the compressive strength of CFST columns. Based on this observation, columns with an outer diameter of D = 504 mm, a steel tube thickness of t = 12 mm, and a height of H = 1764 mm (equivalent to 3.5D) were selected for further parametric studies. The matrix of CFST column specimens used in these studies is presented in Table 1.

All full-scale column models were accurately simulated with variations in key parameters, including loading conditions and material strengths. The results and corresponding discussions are provided in detail in the following section.

Table 1. *A matrix of CFST column specimens*

Specimen	H (mm)	D (mm)	t (mm)	f_s (MPa)	f'_c (MPa)
C-CFE-620-80	1764	504	12	620	80
C-CFE-620-90	1764	504	12	620	90
C-CFE-620-100	1764	504	12	620	100
C-CFE-655-80	1764	504	12	655	80
C-CFE-655-90	1764	504	12	655	90
C-CFE-655-100	1764	504	12	655	100
C-CFE-690-80	1764	504	12	690	80
C-CFE-690-90	1764	504	12	690	90
C-CFE-690-100	1764	504	12	690	100
C-CFC-620-80	1764	504	12	620	80
C-CFC-620-90	1764	504	12	620	90
C-CFC-620-100	1764	504	12	620	100
C-CFC-655-80	1764	504	12	655	80
C-CFC-655-90	1764	504	12	655	90
C-CFC-655-100	1764	504	12	655	100
C-CFC-690-80	1764	504	12	690	80
C-CFC-690-90	1764	504	12	690	90
C-CFC-690-100	1764	504	12	690	100

3. Results and discussions

3.1. Nominal compressive strengths

As previously described, full-scale circular CFST columns with varying material strengths were simulated in ABAQUS [21] under concentric compressive loading for both loading cases: CFE and CFC. These simulations aimed to evaluate and analyze the compressive strength and structural behavior of the CFST columns. The material properties and geometric configurations used in the models are detailed in Table 1 and illustrated in Figure 4.

Table 2. *Nominal compressive strengths of full-scale CFST columns according to AS/NZS 2327: 2017[20]*

D (mm)	t (mm)	A_s (mm^2)	f_s (MPa)	A_c (mm^2)	f'_c (MPa)	N_{us} (kN)
504	12	18548	620	180956	80	23382
504	12	18548	620	180956	90	24559
504	12	18548	620	180956	100	25735
504	12	18548	655	180956	80	24171
504	12	18548	655	180956	90	25347
504	12	18548	655	180956	100	26524
504	12	18548	690	180956	80	24960
504	12	18548	690	180956	90	26136
504	12	18548	690	180956	100	27312

In parallel, the nominal compressive strengths of the CFST columns were calculated based on the AS/NZS 2327: 2017 standard [20], denoted as N_{us}. Table 2 presents the predicted nominal compressive strengths for full-scale circular CFST columns fabricated from steel and concrete materials with different yield and compressive strength

levels. The data presented in Table 2 demonstrate that these composite columns exhibit exceptionally high load-bearing capacity, indicating their suitability for use in high-rise building applications. Their structural performance under significant axial loads suggests that they can effectively support the demands associated with tall structures, contributing to both safety and material efficiency. This makes them a promising option for modern high-rise construction, where strength, stability, and space optimization are critical design considerations.

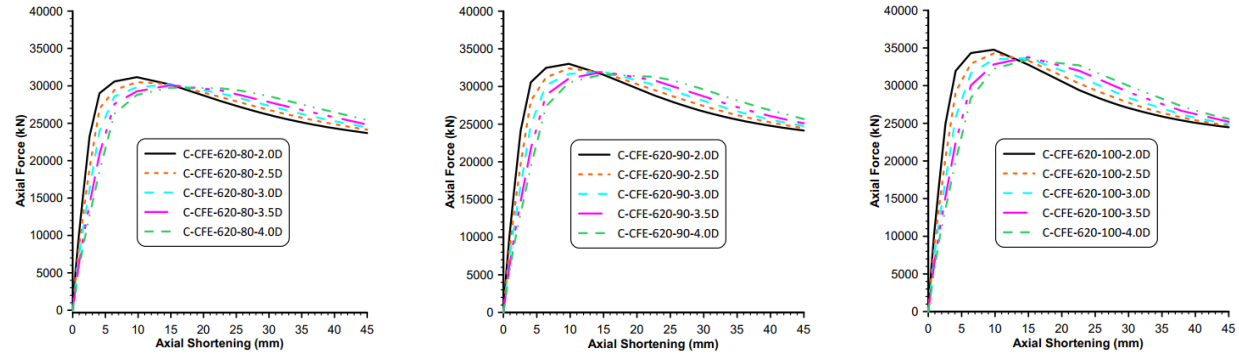

(a) f'_c = 80 MPa *(b) f'_c = 90 MPa* *(c) f'_c = 100 MPa*

Figure 5. *Effect of column height on compressive strength under the CFE loading case*

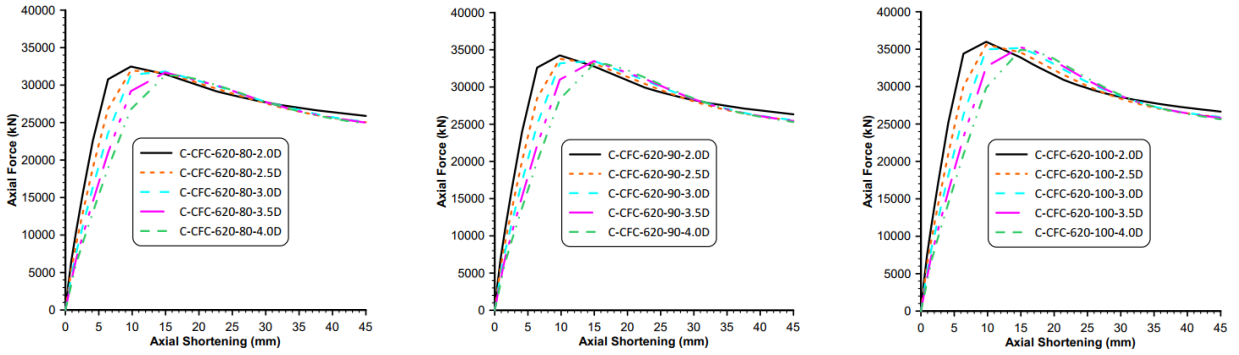

(a) f'_c = 80 MPa *(b) f'_c = 90 MPa* *(c) f'_c = 100 MPa*

Figure 6. *Effect of column height on compressive strength under the CFC loading case*

3.2. FEM results and compressive strength comparisons

The numerical results, including compressive strengths and axial force - axial shortening (P-Δ) relationships for all CFST column specimens, are presented in Table 3 and Figures 7-9, respectively. Furthermore, representative failure modes and compressive damage patterns for selected specimens are illustrated in Figures 10-12 and Figures 13 and 14, respectively.

The compressive strengths of all eighteen column specimens, denoted as P_{max}, were obtained from the simulation results and are summarized in Table 3. In addition, the FEM results for the different loading cases were compared against the corresponding strength predictions based on the AS/NZS 2327: 2017 design code [20].

As shown in Table 3, the compressive strength of the full-scale CFST columns under the CFC loading case consistently surpasses that of the CFE case across all levels of f_y and f_c'. Specifically, the compressive strengths obtained from the finite element simulations exceed the predictions based on AS/NZS 2327: 2017 by approximately 36.7% to 38.2% in the CFC loading case. This notable increase highlights the effectiveness of direct axial loading on the concrete core, which results in near-perfect confinement provided by the surrounding steel tube.

Table 3. *Column compressive strength by FEMs and comparison with AS/NZS 2327: 2017 [20]*

Specimen	Loading case	f_y (MPa)	f'_c (MPa)	P_{max} (kN)	P_{max} /N_{us}
C-CFE-620-80		620	80	30083	1.287
C-CFE-620-90		620	90	31946	1.301
C-CFE-620-100		620	100	33789	1.313
C-CFE-655-80		655	80	30901	1.278
C-CFE-655-90	CFE	655	90	32782	1.293
C-CFE-655-100		655	100	34647	1.306
C-CFE-690-80		690	80	31701	1.270
C-CFE-690-90		690	90	33596	1.285
C-CFE-690-100		690	100	35474	1.299
C-CFC-620-80		620	80	32063	1.371
C-CFC-620-90		620	90	33790	1.376
C-CFC-620-100		620	100	35443	1.377
C-CFC-655-80		655	80	33124	1.370
C-CFC-655-90	CFC	655	90	34912	1.377
C-CFC-655-100		655	100	36654	1.382
C-CFC-690-80		690	80	34113	1.367
C-CFC-690-90		690	90	35939	1.375
C-CFC-690-100		690	100	37737	1.382

In comparison, the CFE loading case yields compressive strength enhancements of approximately 27.0% to 31.3% over the same code-based predictions. This indicates that applying axial compressive load to the entire composite section also mobilizes the confining action of the steel tube on the concrete core, although the confinement effect is somewhat reduced compared to the CFC loading condition.

The results presented in Table 3 further indicate that variations in the configuration of CFST columns significantly influence the load-bearing capacity of high-rise structures. These findings highlight the importance of carefully selecting column configurations based on specific structural requirements. A critical aspect in this context is the connection detail between the steel beam and the CFST column, which must be appropriately designed and adjusted for each configuration. Properly tailored connection designs are essential to ensure efficient load transfer, maintain structural integrity, and optimize the overall performance of the composite system in high-rise applications.

3.3. Axial force – axial shortening responses

The compressive force versus axial shortening (P-Δ) curves for the CFST columns are presented in Figures 7-9, illustrating the comparative results between the CFE and CFC loading cases across different material strength combinations.

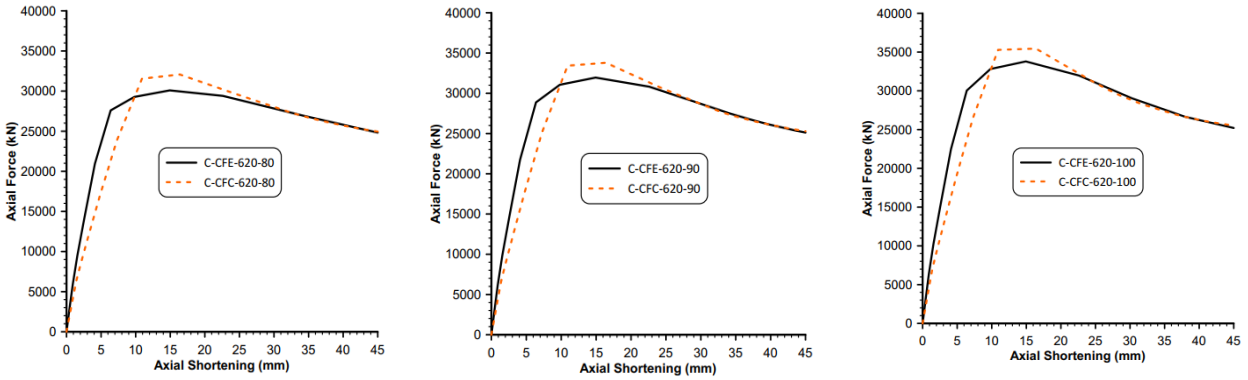

(a) f'_c = 80 MPa *(b) f'_c = 90 MPa* *(c) f'_c = 100 MPa*

Figure 7. *Axial force – axial shortening curves (f_y = 620 MPa)*

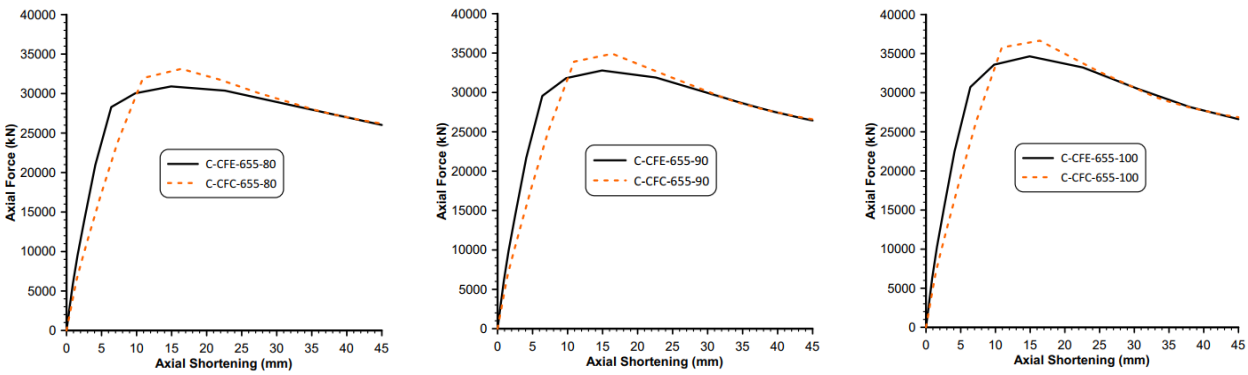

(a) f'_c = 80 MPa *(b) f'_c = 90 MPa* *(c) f'_c = 100 MPa*

Figure 8. *Axial force – axial shortening curves (f_y = 655 MPa)*

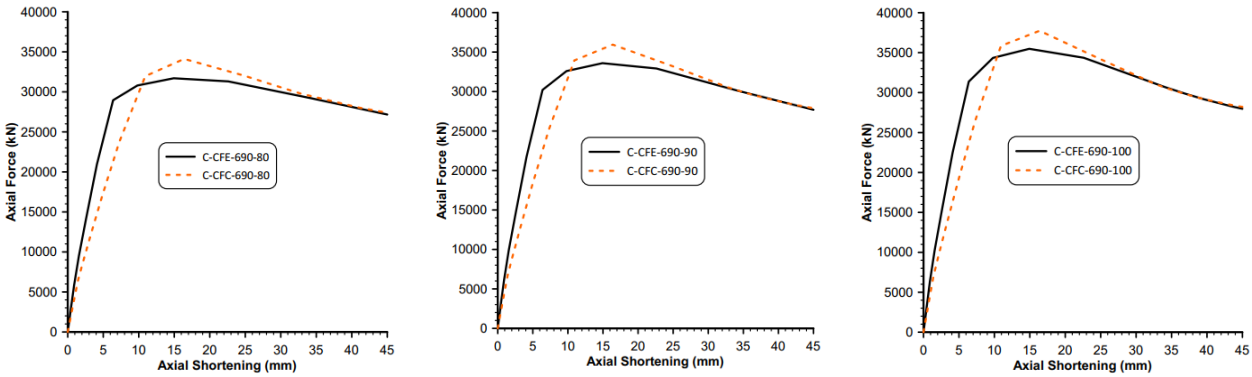

(a) f'_c = 80 MPa *(b) f'_c = 90 MPa* *(c) f'_c = 100 MPa*

Figure 9. *Axial force – axial shortening curves (f_y = 690 MPa)*

Figures 7-9 present the *P-Δ* curves, demonstrating that for all levels of steel yield strength f_y and concrete compressive strength f_c', the CFE loading case exhibits greater compressive stiffness than the CFC loading case during the elastic stage of CFST column behavior. However, this trend reverses in the post-elastic and strength recovery stages. These differences in compressive stiffness between the CFE and CFC loading cases are primarily attributed to variations in the load transfer mechanisms between the steel tube and the concrete core.

During the elastic stage under CFE loading, both the steel tube and the concrete core simultaneously carry the axial load, resulting in a combined stiffness that reflects the contribution of both materials. In contrast, under CFC loading, the concrete core initially bears the axial load directly, with load transfer to the steel tube occurring more gradually. Consequently, the compressive stiffness in this stage is largely governed by the concrete core alone.

In the post-elastic and strength recovery stages, however, the CFST column under CFC loading demonstrates greater stiffness than under CFE loading. This reversal suggests a shift in the structural behavior due to the differing mechanical properties of the constituent materials. Specifically, in the CFE case, the higher Poisson's ratio of steel compared to concrete can reduce the confinement effect the steel tube provides, thereby diminishing the overall compressive stiffness. Conversely, in the CFC case, the restrained lateral deformation of the concrete core enhances the confinement provided by the steel tube. This increased confinement contributes to the observed improvement in both compressive stiffness and strength during the later stages of loading.

Furthermore, analysis of the *P–Δ* curves also indicates that columns subjected to CFC loading exhibit higher compressive strength compared to those under CFE loading. However, this increase in strength comes at the expense of ductility, as the CFC-loaded columns demonstrate a reduced ability to undergo large deformations before failure. This trade-off highlights the need to balance strength and ductility in design, particularly for applications where energy dissipation and deformation capacity are critical, such as in seismic or high-risk load conditions.

3.4. Column failure modes

The failure modes of the column specimens under two different loading cases, using constituent material combinations of f_y = 620 MPa and f_c' = 80 MPa; f_y = 655 MPa and f_c' = 90 MPa; and f_y = 690 MPa and f_c' = 100 MPa, are shown in Figures 10-12. The comparison and analysis of these failures offer valuable insights into the mechanical behavior of CFST columns subjected to various compressive loading cases with high strength materials.

Analysis of the deformation patterns and stress distribution in both the steel tube and concrete core indicates that different compressive loading cases significantly influence the failure modes of the individual components as well as the overall column behavior. Under both the CFE and CFC loading conditions, deformation and stress distribution at the column's mid-height remain nearly symmetrical across the cross-section. However, a notable distinction arises: in the CFE loading case, failure is primarily initiated by the steel tube reaching its yield strength (f_y), accompanied by minor local buckling and limited cracking in the concrete core. In contrast, while the CFC loading case also leads to steel yielding, it is marked by more extensive cracking within the concrete core. Additionally, the compressive stress in the concrete core is higher under CFC loading compared to CFE, despite the use of identical material grades for both the steel tube and concrete core (Figures 10-12).

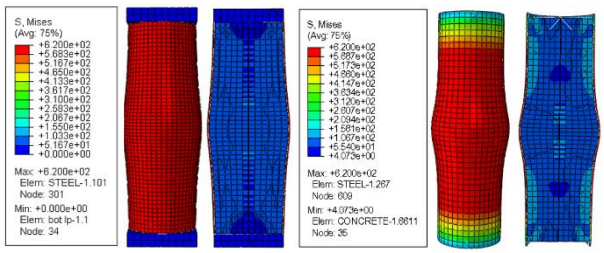

(a) C-CFE-620-80 *(b) C-CFC-620-80*

Figure 10. *Failure modes of the columns with f_y = 620 MPa, f_c' = 80 MPa*

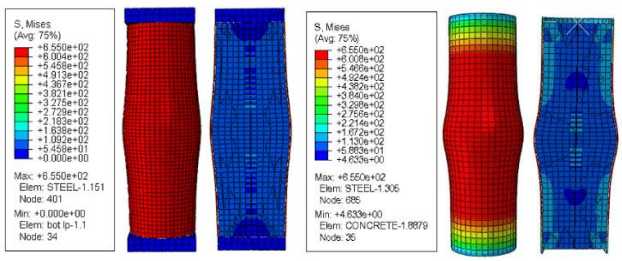

(a) C-CFE-655-90 *(b) C-CFC-655-90*

Figure 11. *Failure modes of the columns with f_y = 655 MPa, f_c' = 90 MPa*

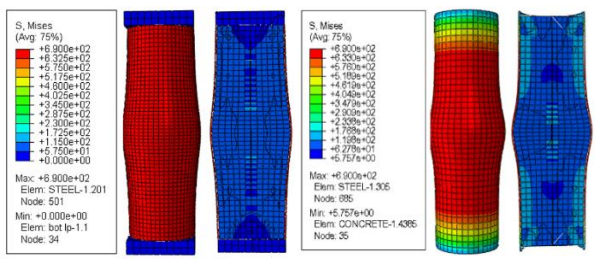

(a) C-CFE-690-100 *(b) C-CFC-690-100*

Figure 12. *Failure modes of the columns with f_y = 690 MPa, f_c' = 100 MPa*

3.5. Compressive damage in the concrete core

Under compressive loading, the concrete core of the CFST columns underwent progressive stages of stress and deformation, culminating in compressive failure at the final stage. Figures 13 and 14 illustrate the compressive damage behavior of the concrete core in CFST columns composed of steel tubes with a yield strength of f_y = 620 MPa and concrete core with compressive strengths ranging from f_c'= 80 to 100 MPa, subjected to two different loading cases: CFE and CFC.

In all cases, the most significant compressive damage was observed at the mid-height of the columns, regardless of concrete strength or loading type. As shown in Figures 13 and 14, increasing the concrete strength f_c' from 80 to 100 MPa resulted in greater maximum compressive damage within the concrete core. This effect was more pronounced under the CFC loading case, where the columns exhibited more severe compressive damage compared to those under CFE loading.

Quantitatively, increasing f_c' from 80 to 100 MPa led to a rise in maximum compressive damage from 0.5997 to 0.6920 for the CFE case, and from 0.6985 to 0.7351 for the CFC case, as derived from the data presented in Figures 13 and 14.

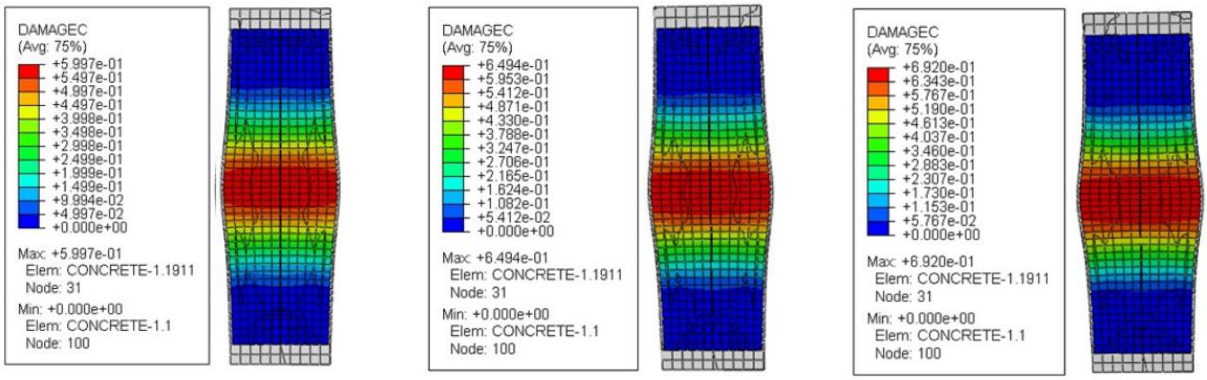

(a) C-CFE-620-80 *(b) C-CFE-620-90* *(c) C-CFE-620-100*

Figure 13. *Compressive damage under the CFE loading case*

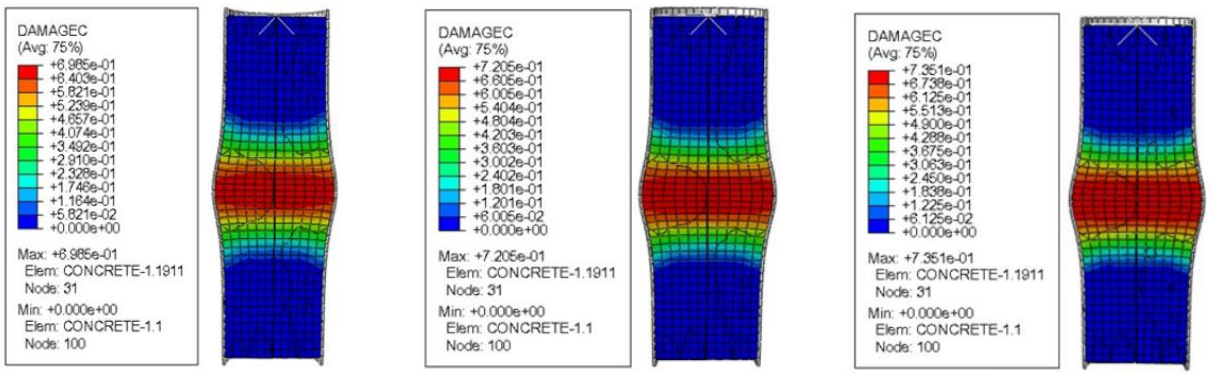

(a) C-CFC-620-80 *(b) C-CFC-620-90* *(c) C-CFC-620-100*

Figure 14. *Compressive damage under the CFC loading case*

4. Conclusions

Based on the numerical simulation results of this study, the following conclusions are drawn:

Column height significantly affects the compressive strength of CFST columns. Therefore, its consideration in the AS/NZS 2327: 2017 design provisions is warranted.

The compressive strength and behavior of CFST columns vary depending on the method of load application. Columns subjected to CFC loading exhibit higher compressive strength than those under CFE loading.

The *P-Δ* curves remain consistent for each loading case as the steel yield strength f_y and concrete compressive strength f_c' increase. During the linear elastic phase, columns under the CFE loading demonstrate greater stiffness. However, beyond the elastic range, the CFC loading case results in higher stiffness and improved strength recovery.

Increasing the steel yield strength f_y and concrete compressive strength f_c' significantly enhances the overall compressive capacity of CFST columns in both loading cases. Despite this increase in strength, the failure modes remain consistent. In the CFE case, failure typically occurs due to steel full-yielding and local buckling, possibly accompanied by concrete cracking. In contrast, failure under the CFC case is initiated by steel partial-yielding and local buckling, followed by more pronounced concrete cracking.

The steel tube provides substantial confinement to the concrete core, enhancing its compressive performance under both loading conditions. This confinement effect is more significant under CFC loading, resulting in higher strength. However, it may also lead to reduced ductility compared to CFE loading.

The most severe compressive damage in the concrete core consistently occurs at the column's mid-height, regardless of material strength or loading type. Columns subjected to CFC loading exhibit more severe internal damage compared to those under CFE loading.

The simulation results indicate that the AS/NZS 2327: 2017 design standard adopts a conservative approach for CFST columns constructed with high strength materials.

Acknowledgments: This work was supported by The University of Danang - University of Science and Technology, code number of Project: T2024-02-09.

REFERENCES

[1] K. Susantha, H. Ge, and T. Usami, "Uniaxial stress–strain relationship of concrete confined by various shaped steel tubes", *Engineering Structures,* vol. 23, no. 10, pp. 1331-1347, 2001. https://doi.org/10.1016/S0141-0296(01)00020-7

[2] M. Johansson and K. Gylltoft, "Mechanical behavior of circular steel concrete composite stub columns", *Journal of Structural Engineering,* vol. 128, no. 8, pp. 1073-1081, 2002. https://doi.org/10.1061/(ASCE)0733-9445(2002)128:8(1073

[3] J. Liu and X. Zhou, "Behavior and strength of tubed RC stub columns under axial compression", *Journal of Constructional Steel Research,* vol. 66, no. 1, pp. 28-36, 2010. https://doi.org/10.1016/j.jcsr.2009.08.006

[4] T. Fujimoto, A. Mukai, I. Nishiyama, and K. Sakino, "Behavior of eccentrically loaded concrete-filled steel tubular columns", *Journal of Structural Engineering,* vol. 130, no. 2, pp. 203-212, 2004. https://doi.org/10.1061/(ASCE)0733-9445(2004)130:2(203)

[5] L.-H. Han, "Flexural behaviour of concrete-filled steel tubes", *Journal of Constructional Steel Research,* vol. 60, no. 2, pp. 313-337, 2004. https://doi.org/10.1016/j.jcsr.2003.08.009

[6] Z.-W. Yu, F.-X. Ding, and C. Cai, "Experimental behavior of circular concrete-filled steel tube stub columns", *Journal of Constructional Steel Research,* vol. 63, no. 2, pp. 165-174, 2007. https://doi.org/10.1016/j.jcsr.2006.03.009

[7] L.-H. Han, W. Liu, and Y.-F. Yang, "Behaviour of concrete-filled steel tubular stub columns subjected to axially local compression", *Journal of Constructional Steel Research,* vol. 64, no. 4, pp. 377-387, 2008. https://doi.org/10.1016/j.jcsr.2007.10.002

[8] H. D. Phan and K.-C. Lin, "Seismic behavior of full-scale square concrete filled steel tubular columns under high and varied axial compressions", *Earthquakes and Structures,* vol. 18, no. 6, pp. 677-689, 2020. https://doi.org/10.12989/eas.2020.18.6.677

[9] Q. Yu, Z. Tao, W. Liu, and Z.-B. Chen, "Analysis and calculations of steel tube confined concrete (STCC) stub columns", *Journal of Constructional Steel Research,* vol. 66, no. 1, pp. 53-64, 2010. https://doi.org/10.1016/j.jcsr.2009.08.003

[10] Z. Tao, Z.-B. Wang, and Q. Yu, "Finite element modelling of concrete-filled steel stub columns under axial compression", *Journal of Constructional Steel Research,* vol. 89, pp. 121-131, 2013. https://doi.org/10.1016/j.jcsr.2013.07.001

[11] H.-T. Thai, B. Uy, M. Khan, Z. Tao, and F. Mashiri, "Numerical modelling of concrete-filled steel box columns incorporating high strength materials", *Journal of Constructional Steel Research,* vol. 102, pp. 256-265, 2014. https://doi.org/10.1016/j.jcsr.2014.07.014

[12] H. D. Phan and H. H. Trinh, "Analysis of mechanical behaviour of circular concrete filled steel tube columns using high strength concrete", in *Mechanics of Structures and Materials XXIV*: CRC Press, 2019, pp. 260-265.

[13] H.-T. Hu, C.-S. Huang, M.-H. Wu, and Y.-M. Wu, "Nonlinear analysis of axially loaded concrete-filled tube columns with confinement effect", *Journal of Structural Engineering,* vol. 129, no. 10, pp. 1322-1329, 2003. https://doi.org/10.1061/(ASCE)0733-9445(2003)129:10(1322)

[14] H. D. Phan, "Numerical analysis of seismic behavior of square concrete filled steel tubular columns" *Journal of Science and Technology in Civil Engineering (JSTCE)-HUCE,* vol. 15, no. 2, pp. 127-140, 2021. https://doi.org/10.31814/stce.nuce2021-15(2)-11

[15] S. Thai, N. H. Cuong, and D. V. Thuat, "Finite element modelling of rectangular concrete-filled steel tube stube columns incorporating high strength and ultra-high strength materials under concentric axial compression", *Journal of Science and Technology in Civil Engineering - HUCE (NUCE)*, vol. 15, no. 4, pp. 74-87, 2021.

[16] H. D. Phan, K.-C. Lin, and H. T. Phan, "Numerical Simulation of Full-Scale Square Concrete Filled Steel Tubular (CFST) Columns Under Seismic Loading", in *Modern Mechanics and Applications: Select Proceedings of ICOMMA 2020*: Springer, 2021, pp. 875-889. https://doi.org/10.1007/978-981-16-3239-6_68

[17] H. D. Phan and K.-C. Lin, "Seismic Performance of Concrete Filled Steel Tubular (CFST) Columns with Variously Axial Compressive Loads", in *Modern Mechanics and Applications: Select Proceedings of ICOMMA 2020*: Springer, 2021, pp. 915-925. https://doi.org/10.1007/978-981-16-3239-6_71

[18] H. D. Phan and L. K. T. Dao, "Numerical analysis of compressive behavior of circular concrete filled steel tubular columns with high to ultra-high strength materials", *Journal of Science and Technology in Civil Engineering (JSTCE)-HUCE,* vol. 17, no. 2, pp. 83-98, 2023. https://doi.org/10.31814/stce.huce2023-17(2)-08

[19] H. D. Phan and T. C. Le, "Mechanical behavior of concrete filled steel tubular columns with high strength materials subjected to various compression loading scenarios", *Journal of Science and Technology in Civil Engineering (JSTCE)-HUCE,* vol. 19, no. 1, pp. 93-107, 2025. https://doi.org/10.31814/stce.huce2025-19(1)-08

[20] *Composite structures – Composite steel-concrete construction in buildings.* Standards Australia/Standards New Zealand, Sydney/Wellington, Australia/New Zealand, AS/NZS 2327: 2017.

[21] SIMULIA, "*Abaqus Analysis User's and Abaqus/CAE User's Guides*", 2016.